Aquatic Sciences (2019) 81:13
https://doi.org/10.1007/s00027-018-0610-3

Aquatic Sciences

RESEARCH ARTICLE

Respiration and aeration by bioturbating Tubificidae alter biogeochemical processes in aquatic sediment

Rémon M. Saaltink[1,8] · Eldin Honingh[1] · Stefan C. Dekker[1,2] · Jasper Griffioen[1,3] · Mariëlle C. van Riel[5,6] · Piet F. M. Verdonschot[5,6] · Jos P. M. Vink[4] · Johan C. Winterwerp[7] · Martin J. Wassen[1]

Received: 26 March 2018 / Accepted: 12 December 2018 / Published online: 19 December 2018

Abstract

This study investigates the potential of bioturbating Tubificidae to alter biogeochemical processes by sediment aeration in order to enhance ecosystem development in eco-engineering projects. We introduced Tubificidae in three different densities (5000, 15,000, and 30,000 individuals m^{-2}) in clay-rich sediment from lake Markermeer (The Netherlands). Redox potential, nutrients and major elements were measured from the water column and porewater at different depths. Mineral phase and redox transfers were chemically modelled and oxygen concentrations in bioturbated sediments for each density were mathematically predicted. The measured results of this experiment showed that Tubificidae oxygenated the upper 15 mm of the sediment. This resulted in decomposition of sedimentary organic matter with an associated sixfold increase in NH_4 and NO_x concentrations in the porewater and the water column. However, phosphorus concentrations were declining in the upper 16 mm, likely as a result of immobilization by pyrite oxidation and production of iron oxides. These bioturbation effects were highest in the treatment with an intermediate density of Tubificidae (15,000 worms m^{-2}) as aeration effects in the treatment with the highest density of Tubificidae (30,000 worms m^{-2}) was impeded by high respiration rates. Furthermore, with a two dimensional diffusion model, simulated effects of respiration and aeration on the oxygen concentration in the sediment suggest that the bioturbation effect is strongest at a density of 12,000 worms m^{-2}. In ecological engineering projects where fast ecosystem development is important, introducing Tubificidae to aquatic sediments to optimal densities might enhance initial ecosystem development due to improved availability of nitrogen as nutrient.

Keywords Eco-engineering · Marker Wadden · Markermeer · Nutrient availability · Oxidation · PhreeqC

Introduction

Bioturbation in aquatic sediments play an important role in regulating geochemical cycling in lakes, rivers and estuaries (Mermillod-Blondin and Rosenberg 2006; Volkenborn et al. 2007). For example, processes like denitrification,

Electronic supplementary material The online version of this article (https://doi.org/10.1007/s00027-018-0610-3) contains supplementary material, which is available to authorized users.

✉ Rémon M. Saaltink
r.saaltink@has.nl

[1] Department of Environmental Sciences, Copernicus Institute of Sustainable Development, Utrecht University, Utrecht, The Netherlands

[2] Faculty of Management, Science and Technology, Open University, Heerlen, The Netherlands

[3] TNO Geological Survey of the Netherlands, Utrecht, The Netherlands

[4] Deltares, Soil and Subsurface Systems, PO-box 85467, 3508 AL Utrecht, The Netherlands

[5] Institute for Biodiversity and Ecosystem Dynamics, University of Amsterdam, P.O. Box 942448, Amsterdam, The Netherlands

[6] Wageningen Environmental Research, Wageningen UR, P.O. Box 47, Wageningen, The Netherlands

[7] Department of Hydraulic Engineering, Delft University of Technology, Delft, The Netherlands

[8] Research Group of Sustainable Production, HAS University of Applied Sciences, 's-Hertogenbosch, The Netherlands

nitrification and iron-sulfur cycling are governed by bioturbators occupying many lake sediments (e.g. Svensson and Leonardsson 1996; Svensson et al. 2001; Lagauzère et al. 2011). Moreover, bioturbation also affects sediment porosity and shear strength, which enhance resuspension of sediment particles (Krantzberg 1985; Sanford 2008). Thus, enhanced turbidity levels in lakes can sometimes be associated with bioturbation activity in the sediment (Krantzberg 1985; De Lucas Pardo et al. 2013).

The bed sediment of lake Markermeer—a shallow artificial lake of c. 700 km^2 in the Netherlands—is occupied by bioturbating macroinvertebrates (Van Riel et al. 2018). These bioturbators formed the soft clay-rich layer that is now covering the bottom of the lake and may resuspend as a result of wind and wave action (Van Kessel et al. 2008; Vijverberg et al. 2011; De Lucas Pardo et al. 2013). The upper few millimeters to centimeters of this layer are in a dynamic equilibrium with the water column, unfavorably affecting the lakes turbidity. Furthermore, a decrease in phosphorus and nitrogen availability reduces primary productivity and adds to a decline in biodiversity (Noordhuis et al. 2014). To improve the ecological conditions in the lake, an innovative project was initiated in which part of the soft clay-rich bed will be dredged and used as building material for approximately 10,000 ha of new wetland within the lake (currently under construction). However, lake Markermeer is nutrient limited with low values of nitrate, ammonium and phosphate in the water column (Noordhuis et al. 2014; Ministry of Infrastructure and the Environment 2017). Hence, ecological development in the littoral zone of these wetlands may be hampered due to limited availability of nutrients.

To minimize total expenditure when building these wetlands, ecological processes will be used to speed up ecosystem development. This method is called ecological engineering and aims to use environmental technology that is tuned to ecosystem services (Mitsch 1998; Odum and Odum 2003; Temmerman et al. 2013). Because the building material (i.e. the soft clay-rich layer) is rich in nitrogen and iron-bound phosphorus (Saaltink et al. 2017), aquatic macroinvertebrates might be introduced to these sediments to actively alter processes in the sediment–water interface and make nutrients available to stimulate plant growth. For example, filter feeders, like *Dreissena burgensis* and *Dreissena polymorpha*, are known to increase phosphorus levels in the water column by mobilizing phosphorus from sediment particles (Turner 2010; Ruginis et al. 2014).

Introducing bioturbating invertebrates to sediments can also be a fruitful method to alter nutrient conditions in the soil and water column (Hansen and Kristensen 1997). The soft clay-rich layer in Markermeer contains about 12,800 invertebrates m^{-2}, of which the Annelida comprise about 40% (c. 5000 individuals m^{-2}) (Van Riel et al. 2018). From these annelids, c. 3900 individuals m^{-2} belong to the subclass Oligochaeta. Bioturbation implies the physical displacement of particles and water by macrofaunal reworking and ventilation (Kristensen et al. 2012). This process is also known as bio-mixing (i.e. solid particle transport) and bio-irrigation (i.e. solute transport). These types of bioturbation can have opposing effects (Van de Velde and Meysman 2016). Oligochaetes like Tubificidae dig tubes and feed with their head downwards, ingesting sediment and water, which pass vertically through the gut and are defaecated as faecal pellets on top of the sediment (Pelegri and Blackburn 1995; Martin et al. 2005). This type of bioturbation is called conveyor belt transport (Fisher et al. 1980). Additionally, the Tubificidae move through the sediment, hereby creating small tubes that extend in different directions in the sediment. Both types of behavior might be important for transporting nutrients from the sediments to the water column. In the following, when we use the term bioturbation, we refer in general to transportation of solutes.

Bioturbating oligochaetes increase the oxygen exchange over the sediment–water interface via irrigation of burrows, which leads to a downward movement of the aerobic zone in the sediment (Krantzberg 1985). These burrows produce a mosaic of oxic and anoxic interfaces as a result of aeration and respiration processes (Kristensen 2000). As many of the biogeochemical processes that occur in saturated sediments are governed by the availability of oxygen, bioturbation leads to changes in nutrient availability (Fillos and Swanson 1975; Callender and Hammond 1982; Vepraskas et al. 2001). Hansen and Kristensen (1997) found that worm activity accounted for up to 46% of the observed increase in nutrient concentrations, indicating enhanced microbial activity in the sediment, which can accelerate the turn-over rate of nutrients. Schaller (2014) showed that apart from nutrients, Mg, Ca and Sr were also highly affected by bioturbation, whereas Al, Fe, Co, Cu, Mn, and Zn were affected only to a small extent. The above results demonstrate the importance of bioturbation in geochemical cycling in lake, river and marine sediments (Volkenborn et al. 2007; Vink 2009).

The overall effect of bioturbators on the biogeochemical processes depends on the characteristics of the sediment, environment, and benthic communities which are involved. To investigate the potential effect of bioturbating Tubificidae on the nutrient availability in the littoral zone to be constructed by the soft clay-rich sediment from lake Markermeer, we need to know how bioturbation alters biogeochemical processes in the topsoil. Since the impact of bioturbation on biogeochemistry depends on bioturbation activity, we carried out a microcosm experiment with different densities of Tubificidae to identify the effects on biogeochemical processes in porewater. We monitored porewater chemistry at different depths in the soft clay-rich layer as well as surface water. We hypothesize that bioturbation

positively influences nitrogen exchange to the water column by changing the oxidation state of the sediment. However, we also expect that the altered oxidation state will lead to immobilization of phosphorus by binding with iron oxides, as sediments from lake Markermeer are rich in pyrite, which would be subject to oxidation.

Methods

Experimental set-up

This study was performed with an experimental technique (EU-patent nos. 1018200/02077121.8, October 2001, J. Vink, Rijkswaterstaat), which was introduced as Sediment Or Fauna Incubation Experiment, or SOFIE® (Vink 2002; http://www.sofie.nl). This sampling device consists of a circular two-compartment cell (190 mm radius, 200 mm height). We used two two-compartment SOFIE®-devices to allow for simultaneous testing of four treatments. Each compartment was filled with soft sediment from the northern part of lake Markermeer. See Table 1 for the sediment properties of the soft clay-rich layer used in this study. This sediment was stored in dark air-tight containers at 4 °C prior to the start of the experiment. Porewater probes, constructed from a 0.1 µm-permeable polyethersulfone polymer (X-flow Industries, Almelo, The Netherlands), were installed in gastight connectors at a depth of 1, 6, 11, 16, 21, 31, 41 and 51 mm below sediment surface. In addition, one probe was installed 9 mm above the sediment surface to extract a sample from the water column. The probes were positioned in a circular manner in such a way that no interference among probes would occur during sampling.

The SOFIE®-devices were placed in a dark, climate-controlled chamber at 12 °C and were incubated for 4 months to allow stabilization of chemical processes after sediment disturbance. Two-Ampere electric pulses were applied biweekly in each compartment in the first 2 months of the 4-month incubation period to clear the sediments of any macroinvertebrates. After about 6 weeks, no activity related to bioturbation could be identified in the cells. At the start of the experiment Tubificidae were added to three of the four compartments at different densities: 5000, 15,000 and 30,000 Tubificidae per m^2 surface (these treatments are hereafter referred to as T_{5k}, T_{15k} and T_{30k}). These Tubificidae were bought in The Netherlands (EAN: 4038358100154) and most likely can be classified as *Limnodrilus* spp., present in varying sizes. The fourth compartment contained no Tubificidae and thus functioned as our control treatment. Because Annelids in lake Markermeer occur at densities of c. 5000 individual m^{-2} (Van Riel et al. 2018), the treatments used in this study allow to analyze differences in chemical processes in the sediment with increasing densities of bioturbating annelids compared to the field situation.

Table 1 Geochemical and mineralogical composition of the sediment used in this study, with mean concentrations in dry wt with standard deviations ($n=5$). Adapted from Saaltink et al. (2018)

	Unit	n	Mud	SD
Aqua regia/CS/CN				
Al	mg kg^{-1}	5	10,398	219
Ca	mg kg^{-1}	5	48,058	1288
Fe	mg kg^{-1}	5	14,766	234
K	mg kg^{-1}	5	2619	72
Mg	mg kg^{-1}	5	5106	135
Mn	mg kg^{-1}	5	360	10
N	mg kg^{-1}	5	1611	32
Na	mg kg^{-1}	5	97	34
P	mg kg^{-1}	5	361	10
S	mg kg^{-1}	5	4513	187
Sr	mg kg^{-1}	5	113	3
Ti	mg kg^{-1}	5	396	17
Zn	mg kg^{-1}	5	130	3
SEq. P extraction				
Exchangeable P	mg kg^{-1}	5	5	2
Fe-bound P	mg kg^{-1}	5	40	10
Ca-bound P	mg kg^{-1}	5	89	18
Detrital P	mg kg^{-1}	5	158	14
Organic P	mg kg^{-1}	5	47	11
Fe as oxides	mg kg^{-1}	5	851	39
XRD				
Quartz	%	1	45.8	
Plagioclase	%	1	8.2	
Alkali feldspar	%	1	3.7	
Calcite	%	1	11.9	
Dolomite	%	1	2.8	
TiO_2	%	1	0.4	
Pyrite	%	1	1.0	
Phyllosilicates	%	1	26.3	
Other				
Organic matter	%	5	4.0	0.1

Sample analysis

Porewater and surface water were collected from the probes on days 0, 7, 14 and 28. Chloride, NO_2, NO_3 and SO_4 were determined using ion chromatography (IC); Ca, Fe, K, Mn, Na, Si and Sr were determined with Inductively Coupled Plasma Optical Emission Spectrometry (ICP-OES), ammonium was determined with the phenol-hypochlorite method (Helder and De Vries 1979), PO_4 with the ammonium-heptamolybdate method (Kitson and Mellon 1944) and pH by an ion-specific electrode. The porewater volume extracted from

the rhizons did not exceed 4 ml to minimize the disturbance of the internal water balance in the sediment. Redox potentials (Eh) were measured with a 1.6 × 40 mm needle sensor (RD-NP, Unisense), inserted through the sediments surface and 1 mm resolution profiles were made with a microprofiling system (Unisense).

The length of Tubificidae burrows at each depth were determined from pictures taken at day 7, 14 and 28. A specific section of the cell wall (3 cm wide, 10 cm long) was analysed from the photographs. We assume that the Tubificidae densities determined from these photographs are representative for the entire cell-compartment. Burrow length was calculated with SmartRoot in Image J (Lobet et al. 2011), which is especially designed for analyzing plant roots. As the contrast between burrow holes and undisturbed sediment was high enough for the software to make a distinction, we deemed this method suitable for determining the length of the burrows.

Statistical analysis

A robust factor analysis was used to determine main relationships between aqueous concentrations and sediment properties within the three Tubificidae treatments. This method was chosen over a classical factor analysis because direct application of multivariate statistical analysis to compositional (closed) data might give a wrong impression (Filzmoser et al. 2009). Compositional variables from the dataset were first assessed with the isometric logratio transformation (ilr-transformation) (Egozcue et al. 2003). With these data, a robust estimation was obtained of the covariance matrix, after which the data were back transformed to the centered logratio (clr) space. This set of transformations was only done for the variables expressed as concentrations. Thus, depth and Eh were transformed with a normal logratio transformation. The transformed dataset was used for the parameter estimation in factor analysis. For a full description of this method, we refer to Filzmoser et al. (2009). The modeling script for computing the robust factor analysis is added in the supplement.

Modelling

Modeling phase transfers and redox transfers

To identify chemical processes that occurred between two measurement points in time, we used inverse modelling in the PHREEQC program (Parkhurst and Apello 2013). Inverse modeling calculates possible mole transfers of minerals and gases that explain the change in chemical composition of two solutions. The outcome of the PHREEQC inverse model simulations depends on the (pre)selected mineral phases. In this paper, the selected mineral phases are based on the mineralogical analysis presented in Table 1 and on biogeochemical processes identified in the same type of sediment by Saaltink et al. (2016). The PHREEQC software is based on mass-balance equations of preselected mineral phases (reactants). The mineral phases can either precipitate (leave the solution) or dissolve (enter the solution), expressed in mole transfers. Comparably, gases can either be consumed or released (leave the solution) or be taken up (enter the solution). Van der Grift et al. (2016) showed that iron hydroxyphosphates ($FePO_4(OH)$) can precipitate upon oxidation in pH-neutral groundwater in presence of dissolved Fe(II) and PO_4. To allow precipitation and dissolution of iron hydroxyphosphates, we added this phase to the PHREEQC database, using the solubility constant after Luedecke et al. (1989): $Log\ K[Fe_{2.5}PO4(OH)_{4.5}] = -96.7$. The other mineral phases that we selected for inverse modelling are calcite, hydroxyapatite, iron oxyhydroxides, pyrite, O_2 (g), CO_2 (g), and H_2O (g). We applied inverse modeling between day 0 and 7, day 7 and 14 and day 14 and 28 in which all possible combinations of the mass-balance equations are accepted within a range of measured porewater concentrations ± 5%.

To enable the model to attribute some of the chemical changes to cation-exchange processes, we included an assemblage of exchangers (X): KX, MgX_2, MnX_2, NaX and NH_4X. The sum of this assemblage was defined as the cation-exchange capacity (CEC) calculated from the sediment composition, which was 30 meq 100 g^{-1} (Saaltink et al. 2016). The cation-exchange capacity is important to take into account, since it describes the buffering of some of the chemical processes in sediments by adsorption or desorption of cations. Likewise, redox transfers are modelled for Fe, N, O, and S, that can either oxidize or reduce.

Simulations explaining changes in water chemistry via phase and redox transfers were computed for 6, 21 and 51 mm depth for each treatment. For every situation, several valid simulations were found due to small differences in the amount of mole transfers attributed to the mineral phases. Here, we present the plausible simulation with the smallest amount of mole transfers. As an example, we have added the inverse model PHREEQC-script for the T_{5k} treatment between t = 0 and t = 7 days in the supplement.

Modeling aeration and respiration

An equilibrium 2D diffusion model was created to explain the combined effect of aeration and respiration by bioturbating Tubificidae. It is important to note that this equilibrium model is explaining diffusion and respiration processes in a general manner, ignoring that in situ many coefficients in this model would be affected by changing factors such as temperature of the water, wave action and even the species of Tubificidae. Moreover, the model could potentially

underestimate the aeration potential by bioturbation, as it excludes two mechanisms: (1) peristaltic-like movements of Tubificidae that could in theory stimulate water movement in the tube; and (2) faecal pellet deposition that could result in passive irrigation of the tubes.

We schematize the role of Tubificidae in the sediment core as a burrow in the form of a cylinder. Through this burrow, oxygen can penetrate easily and is diffused into the sediment from the edge of this burrow, inducing an oxygen-rich cylinder. However, with increasing number of Tubificidae, the entire sediment surface becomes occupied and Tubificidae will move around, cross each other and curl together or fill the voids in between the oxygen-rich cylinders. Hence, the assumption that the number of Tubificidae scales linear with aeration is valid up to a critical number of Tubificidae. We assume that more Tubificidae will not increase the oxygen content in the sediment anymore. The aerated sediment volume as a function of the number of Tubificidae will roughly follow a tangent-hyperbolic function, as shown in Fig. 1b. Tangent-hyperbolic functions effectively capture many saturation curves that occur in nature (e.g., Oates 1985; Walker et al. 2011).

Furthermore, n Tubificidae consume nR_T amount of oxygen per unit time, where R_T is the respiration rate per Tubificidae. Note that nR_T and R_T reflect average values from literature; it is likely that these values change continuously in reality due to changes in activity, stress and water temperature. Depending on the aeration and respiration rate, the aeration and respiration curves can intersect. Likely, the oxygen concentration in the sediment initially increases with the number of Tubificidae and then decreases. We presume that the oxygen concentration yields the balance between respiration by n_* Tubificidae per burrow, and the flow of oxygen from the ambient water by diffusion ($O_{2,a}$). This diffusion is governed by the diffusion coefficient D_a of ambient water and the sediment (D_s). The abovementioned processes were included in a mathematical model, of which the final equilibrium equation reads:

$$\langle O_{2,s} \rangle = \frac{O_{2,a}}{4} - \frac{n_* R_T}{24 D_a} \delta_T^2 - \frac{R_0}{12 F(n) D_s} \delta_T^2 \quad (1)$$

This mathematical model is extensively explained in the supplement. Eq. (1) shows that there is an optimum in the mean oxygen concentration in the sediment $\langle O_{2,s} \rangle$ as a function of the number of Tubificidae n and their burrow function F(n).

Results

Experimental results

Effects of bioturbation on N, P, and Eh

Figure 2 presents depth profiles of all four treatments at experimental time t = 28 days. The length of the Tubificidae burrows (Fig. 2a) decreased with depth for all three densities. The Tubificidae density effect on burrow length between T_{15k} and T_{30k} was only prevalent in the upper

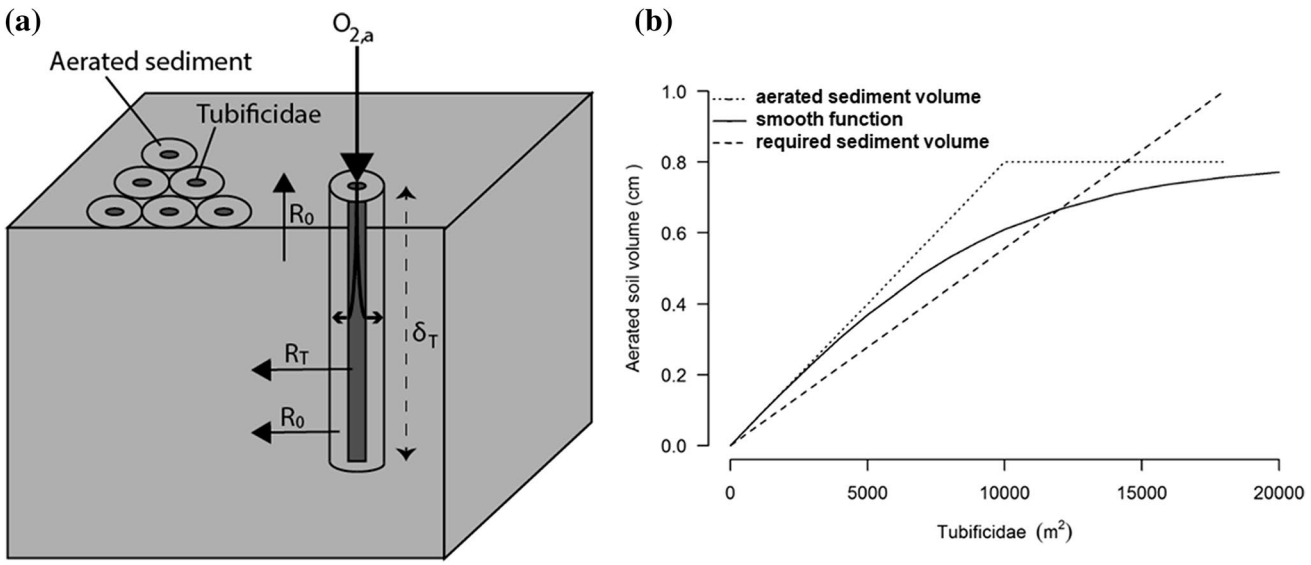

Fig. 1 **a** Conceptual overview of the aeration processes used in the model in which $O_{2,a}$ is the oxygen flow in the burrow into aerated sediment, R_0 is the sediment respiration and R_T is the respiration rate per Tubificidae, **b** a diagram of the oxygen balance in the sediment: the aerated volume as a function of number of Tubificidae, its tangent hyperbolic approximation (F(n)), and the oxic sediment volume required for the respiration of n Tubificidae

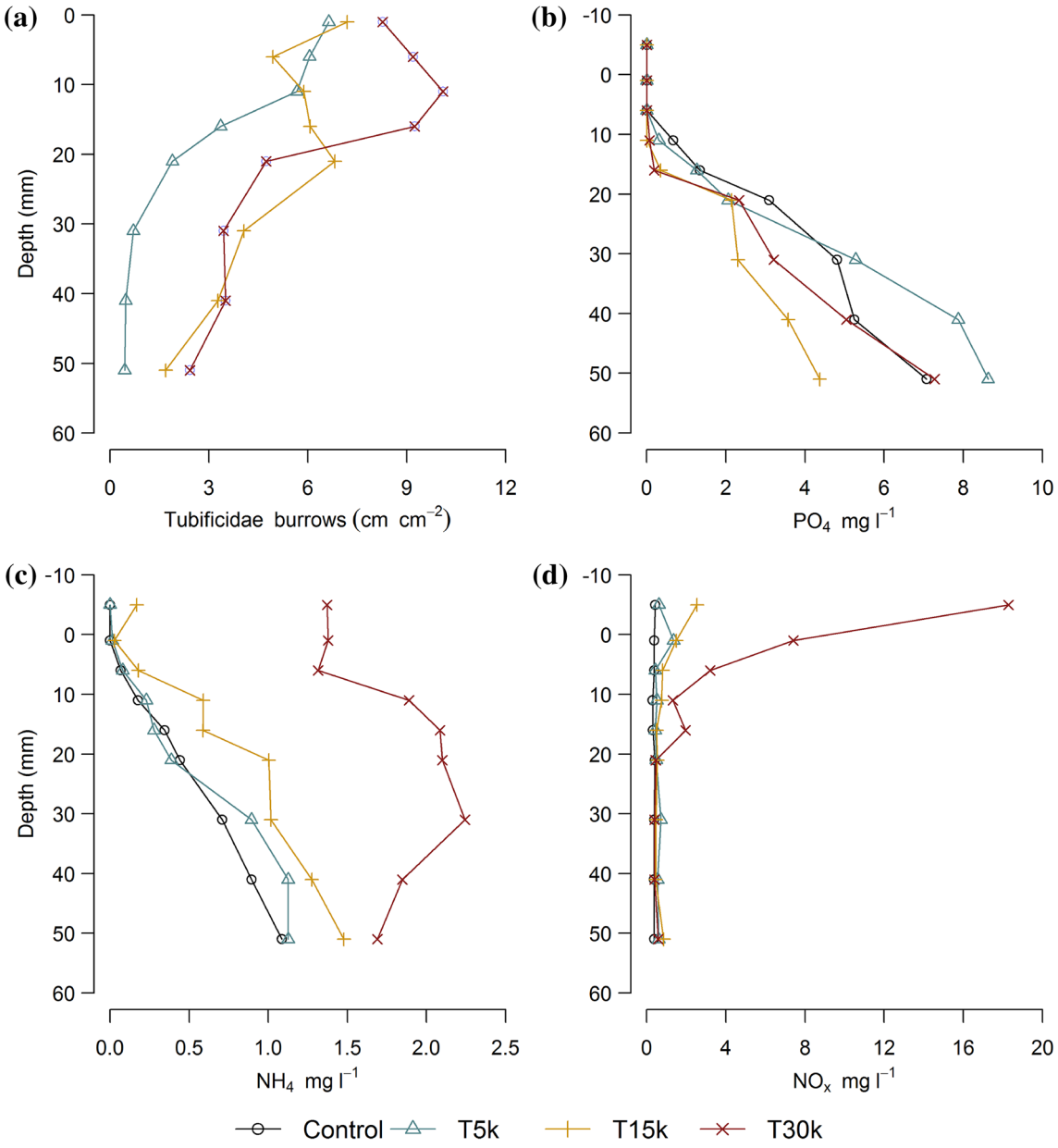

Fig. 2 Measured depth profiles of Tubificidae burrows (cm) (**a**), PO_4 (**b**), NH_4 (**c**) and NO_x (**d**) in mg l^{-1} for the control treatment as well as T_{5k}, T_{15k} and T_{30k}

20 mm ($p < 0.05$), while the burrow length in T_{5k} was less than T_{15k} and T_{30k} down to 50 mm below sediment surface ($p < 0.05$).

Marginal changes in PO_4 concentrations were found between the treatments (Fig. 2b) ($p < 0.05$ for all treatment combinations, except between the control and T_{30k}). As expected, PO_4 concentrations increased with increasing depth as presence of oxygen immobilizes phosphorus in iron-rich clay sediments. In the Tubificidae treatments, PO_4 was immobilized in the upper 11–16 mm, while P immobilization in the control occurred only in the upper 6 mm.

Nitrogen in the sediment was highly affected by bioturbation (Fig. 2 c,d). Ammonium concentrations in T_{15k} and T_{30k} were higher than in the control ($p < 0.05$ at 6, 11, 16, 21, 31, 41, and 51 mm depth for T_{15k} and $p < 0.05$ at 1, 6, 11, 16, and 21 mm depth for T_{30k}). As with PO_4, NH_4 is expected to increase with increasing depth, but this is not the case for T_{30k}, where concentrations were dropping rapidly from 30 to 50 mm depth. Moreover, both T_{15k} and T_{30k} showed elevated NH_4 concentrations in the surface water compared to the control (0.17 and 1.37 mg l^{-1}, respectively; $p < 0.05$ for T_{30k}). In all Tubificidae treatments, elevated NO_x

concentrations in the surface water were found (0.61 mg l^{-1} for T_{5k}, 2.54 mg l^{-1} for T_{15k}, and 18.3 mg l^{-1} for T_{30k}) compared to the control (0.43 mg l^{-1}) ($p < 0.05$ for T_{15k} and T_{30k}). Nitrate/Nitrite concentrations decreased rapidly with increasing depth and were almost zero below a depth of 20 mm.

The effect of bioturbation on the redox potential (Eh) is presented in Fig. 3. Bioturbation resulted in a downward movement of the shift from oxidized to reduced sediment conditions, especially at a depth of 16 mm and lower ($p < 0.001$ for all treatments). The largest shift was seen for T_{15k}, while T_{5k} and T_{30k} were more or less the same and were in between the control treatment and T_{15k}. However, T_{30k} in the upper 16 mm decreased the Eh by approximately 30 mV compared to T_{5k} and T_{15k} ($p < 0.001$), likely by high worm respiration.

These results clearly show that bioturbation by Tubificidae alters Eh and nitrogen concentration in both the porewater and surface water significantly, while only a marginal immobilizing effect was found for PO_4.

Aeration and respiration factors related to bioturbation

The summary output of the robust factor analysis for the three Tubificidae treatments is presented in Table 2. Factor loadings with explained variance are presented in the supplement. Both a respiration factor and an aeration factor by Tubificidae were identified from the relationship between Eh, burrow length and time. The respiration factor explained the largest part of the variance in the dataset (61.3% in T_{5k} and T_{15k}, 68.1% in T_{30k}) and is described by an inverse relationship between the burrow length and time with Eh; as burrow length increases through time, Eh decreases as a result of oxygen consumption. The second most important factor is related to aeration by Tubificidae and is described by a positive relationship of time, burrow length and Eh. This aeration factor is largest for T_{15k} (27.4%), followed by T_{5k} (25.8%). However, this factor was absent in T_{30k}, most likely due to high oxygen consumption, as it is expected that total respiration scales linearly with the number of Tubificidae in the sediment. The results of this analysis suggest that the respiration effect was largest in T_{30k}, while the aeration effect was largest in T_{15k}, in line with the hypothesis presented in "Modeling aeration and respiration".

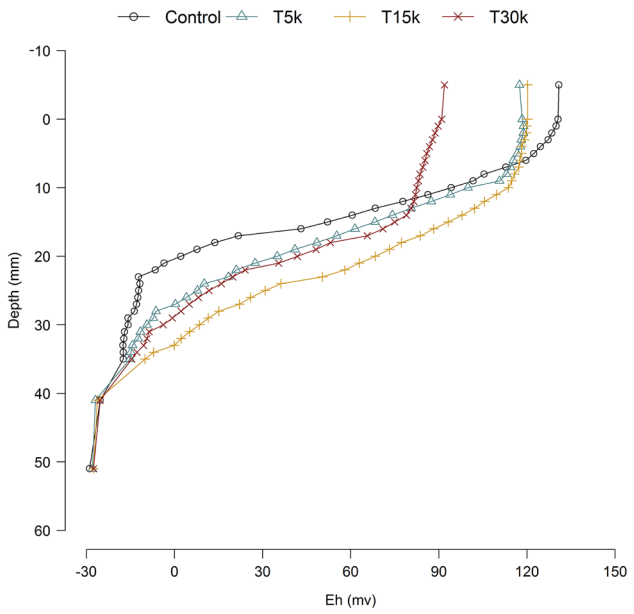

Fig. 3 Measured depth profile of Eh (mV) for the control treatment as well as for T_{5k}, T_{15k} and T_{30k}

Modeled results

Effects of bioturbation on phase and redox transfers

Main phase and redox transfers at 6, 21 and 51 mm depth are depicted in Table 3. The models show that dissolution of calcite ($CaCO_3$) and pyrite (FeS_2) and precipitation of iron hydroxyphosphate ($FePO_4$) are important phase changes in the sediments with Tubificidae, suggesting that sediment aeration caused by bioturbation initiated these processes. The occurrence of these three processes together makes sense as oxidation of pyrite immobilizes phosphate by producing PO_4-bearing Fe hydroxides, sulfate and protons, in turn promoting dissolution of calcite. This potentially affect bioturbation activity and speciation of chemical compounds. Dissolution and precipitation of apatite ($Ca_5(PO_4)_3OH$) and iron(III) hydroxide ($Fe(OH)_3$) were less important and these processes also occurred in the control (Table 3).

When analyzing respiration and aeration effects on bioturbation, modeling redox transfers can give valuable information. As expected, the net redox transfer in the control treatment is low at all three depths (Table 3). In the first week of the experiment, a positive net change in redox transfers was observed in all Tubificidae treatments (191 µmol electrons l^{-1} day^{-1} in T_{5k} at 21 mm depth; 152 µmol electrons l^{-1} day^{-1} in T_{15k} at 6 mm depth; 88 µmol electrons l^{-1} day^{-1} in T_{30k} at 21 mm depth). After the first week, the net redox change remained positive for T_{5k} and T_{15k}, and became negative for T_{30k}, except at 51 mm, where the net redox change became negative after 2 weeks.

The findings presented in Table 3 suggest that several chemical processes are altered by bioturbation. In line with Fig. 3 and Table 2, inversely modeling of redox transfers showed that there is a net oxidation effect for T_{5k} and T_{15k}, while a net reduction effect was found for T_{30k}.

Table 2 Output of robust factor analysis for the four treatments used in this study

Factor	% of explained variance		Sign. positive loadings		Sign. negative loadings	Interpretation
T_{5k}						
1	61.3	$r>0.7$	Cl, Mg, Na, Sr, K, SO_4, pH, Ca, Si, Fe, Eh	$r<-0.7$	Time	Respiration by Tubificidae
		$r>0.5$	NO_x	$r<-0.5$	Burrows	
2	25.8	$r>0.7$	Depth, PO_4, NH_4	$r<-0.7$	Burrows	Aeration by Tubificidae
		$r>0.5$	Mn, Fe	$r<-0.5$	Time, Eh	
3	4.4	$r>0.7$		$r<-0.7$		
		$r>0.5$		$r<-0.5$	Mn	
T_{15k}						
1	61.3	$r>0.7$	Cl, Na, Mg, SO_4, Sr, K, Si, pH, Ca, Fe	$r<-0.7$	Time, burrows	Respiration by Tubificidae
		$r>0.5$	Eh	$r<-0.5$		
2	27.4	$r>0.7$	Mn, NH_4, PO_4, Depth	$r<-0.7$	NO_x	Aeration by Tubificidae
		$r>0.5$		$r<-0.5$	Burrows, time, Eh	
3	5	$r>0.7$		$r<-0.7$		
		$r>0.5$	Eh	$r<-0.5$		
T_{30k}						
1	68.1	$r>0.7$	Cl, SO_4, Mg, Na, Sr, pH, K, Ca, Fe, Si, Mn	$r<-0.7$	Time, burrows	Respiration by Tubificidae
		$r>0.5$	Eh	$r<-0.5$		
2	20.6	$r>0.7$	NO_x	$r<-0.7$	PO_4, depth	Depth effect; NO_x
		$r>0.5$	Eh	$r<-0.5$	Mn	
3	6.1	$r>0.7$		$r<-0.7$	NH_4	
		$r>0.5$		$r<-0.5$		

A distinction is made between positive and negative loadings. Loading coefficients (r) between 0.5 and −0.5 are not shown

Computed oxygen concentrations in bioturbated sediments

The aforementioned results show that bioturbation results in aeration of the sediments. However, due to respiration by Tubificidae, the net aeration depends on the number of Tubificidae per unit area. This was modeled, assuming that the relation between the number of Tubificidae and aerated sediment volume follows a tangent-hyperbolic function. From the aerated sediment volume for the three Tubificidae densities used in this experiment, this relation could be calibrated, yielding $V = 0.80 \tanh(n)$. With this function and the parameter input presented in Table 4, the oxygen concentration in the sediment for a given Tubificidae density was modeled using Eq. (1). Figure 4b presents the computed oxygen concentration for Tubificidae densities between 0 and 40,000 individuals m^{-2}, showing an optimum at 12,000 individuals m^{-2} with an oxygen concentration of 0.85 mg l^{-1} at 1 cm depth. The O_2 concentration quickly decreases with increasing depth, becoming zero below 3 cm depth. Moreover, these results show that there is an aeration effect at 1 cm depth with a Tubificidae density between 4000 and 32,000 individuals m^{-2}. However, as already outlined, the model is simplified in such a way that some variables (e.g. water temperature and associated changes in oxygen concentration in ambient water) are kept constant, which do change in reality. In supplementary Fig. 2, the effect of changing oxygen concentrations in ambient water—driven by seasonal changes in temperature—on the oxidation effect by Tubificidae is elaborated.

This model output explains the results presented in "Experimental results"and "Modeled results" by showing that T_{15k} is closest to the optimal aeration effect. It furthermore explains why reduced conditions are found in all treatments below a depth of 33 mm (Fig. 3).

Discussion

This study shows that bioturbation by Tubificidae effectively aerated the upper layer of the sediment. The largest aeration effect was discerned at a density of 15,000 worms m^{-2}. This becomes evident from our experiment (Fig. 3), where a downward movement of the shift from oxidized to reduced sediment conditions is apparent at a depth of 16 mm and lower. Moreover, both the factor analysis and the modeled redox transfers suggest highest aeration effects in the T_{15k} treatment (Tables 3, 4). This conclusion is further supported

Table 3 Phase and redox changes expressed in mole transfers (μmol l^{-1} day^{-1}) as modeled by PHREEQC

Treatment	Depth	Phase transfers						Redox transfers				
		$Fe(OH)_3$	$FePO_4$	$CaCO_3$	$CaPO_4$	FeS_2	CO_2	Fe	N	O	S	ΣRedox
Depth: 6 mm												
Control	Day 0–7		0.6		−0.3		−0.6		0.1		−0.1	0.0
	Day 7–14	−0.2			0.2			−0.2				−0.2
	Day 14–28				−0.4							
T_{5k}	Day 0–7	0.1										
	Day 7–14								0.3	1.3		1.7
	Day 14–28			26		25	−26		0.8	181	51	232
T_{15k}	Day 0–7		−9.1	32	2.6	22	−32	−23	2.0	173		152
	Day 7–14					0.4		0.2	−0.1	2.1	0.7	3.0
	Day 14–28		−5.1	17	1.7	13	−17	−13	−0.2	96	26	108
T_{30k}	Day 0–7		−2.3	23		5.3	−23	−3.9	16	102	11	125
	Day 7–14		0.1			−1.4		−0.4	1.0	−5.4	−2.8	−7.5
	Day 14–28	−1.5				2.1		−2.3	−4.0		4.3	−2.1
Depth: 21 mm												
Control	Day 0–7		−1.8	4.1	−1.3		−4.1	−4.2	−0.5			−4.8
	Day 7–14											
	Day 14–28		−0.1		0.2			−0.2	0.1		−0.1	−0.3
T_{5k}	Day 0–7		−8.2	28	3.3	22	−28	−21	0.9	167	44	191
	Day 7–14		−3.4	12		8.5	−12	−8.5	−1.5	58	17	65
	Day 14–28							0.3		1.3		1.7
T_{15k}	Day 0–7		−0.9	12		5.1	−12	−2.3	4.6	57	10	68
	Day 7–14											
	Day 14–28				0.2			−0.3	0.0			−0.4
T_{30k}	Day 0–7			17		1.4	−17	0.1	15	70	2.7	88
	Day 7–14				−1.5			0.1	−2.0	−7.9		−9.8
	Day 14–28					−0.8			0.3	−4.4		−4.1
Depth: 51 mm												
Control	Day 0–7											
	Day 7–14											
	Day 14–28				−0.4							
T_{5k}	Day 0–7											
	Day 7–14											
	Day 14–28								0.6	2.5		3.2
T_{15k}	Day 0–7											
	Day 7–14							0.0	0.8	3.2		4.0
	Day 14–28		−3.9	13		9.3	−13	−9.7	−2.1	61		50
T_{30k}	Day 0–7											
	Day 7–14					1.1			0.9	11	2.2	14
	Day 14–28								−0.6	−2.3		−2.9

Positive values indicate dissolution for minerals and uptake for gases, negative values indicate precipitation for minerals and release for gases

by the model outcomes of the respiration and oxidation rates of bioturbating Tubificidae (Fig. 4). That model predicts an optimum of 12,000 worms m^{-2}, which is close to the T_{15k} treatment in our experiment. Furthermore, the model showed that the effect of bioturbation on oxidation first increases with increasing densities and then, after the optimum density of 12,000 worms m^{-2} is exceeded, the aeration effect of Tubificidae diminishes as burrows start overlapping geometrically, while the respiration rate per worm stays the same. These opposing mechanisms explain why oxygen concentrations follows an optimum curve with increasing worm density. Likewise, these mechanisms also explain why Eh values decreased in the upper 16 mm in the T_{30k} treatment (Fig. 3) and why no aeration effect was distinguished by

Table 4 Input parameters to model the mean oxygen concentration $<O_{2,s}$ (mg l^{-1})$>$ in the sediment

Parameter	Description	Value/function	Source
$O_{2,a}$	Oxygen concentration in ambient water	11.5 mg l^{-1}	Ministry of Infrastructure and the Environment (2017)
n	Number of Tubificidae	5 k, 15 k, 30 k m^2	From experiment
R_T	Respiration rate per Tubificidae	0.0250 mg hr^{-1}	Fowler and Goodnight (1965), Lou et al. (2013)
F(n)	Burrow function	0.80 tan h(n)	From experiment
δ_T	Mean burrow length	1 cm: 8.35 cm 2 cm: 4.35 cm 3 cm: 2.74 cm 4 cm: 2.42 cm 5 cm: 1.52 cm	From experiment
d_T	Diameter of burrow	0.05 cm	Rogaar (1980)
δ_O	Thickness of oxic layer	0.2 cm	De Lucas Pardo (2014)
D_a	Diffusion coefficient ambient water	0.153 cm^2 h^{-1}	Han and Bartels (1996)
D_s	Diffusion coefficient sediment	0.082 cm^2 h^{-1}	Ullman and Aller (1981) and Iversen and Jørgensen (1993)
R_0	Respiration rate of sediment	0.0205 cm^2 h^{-1}	From supplement equation (2)

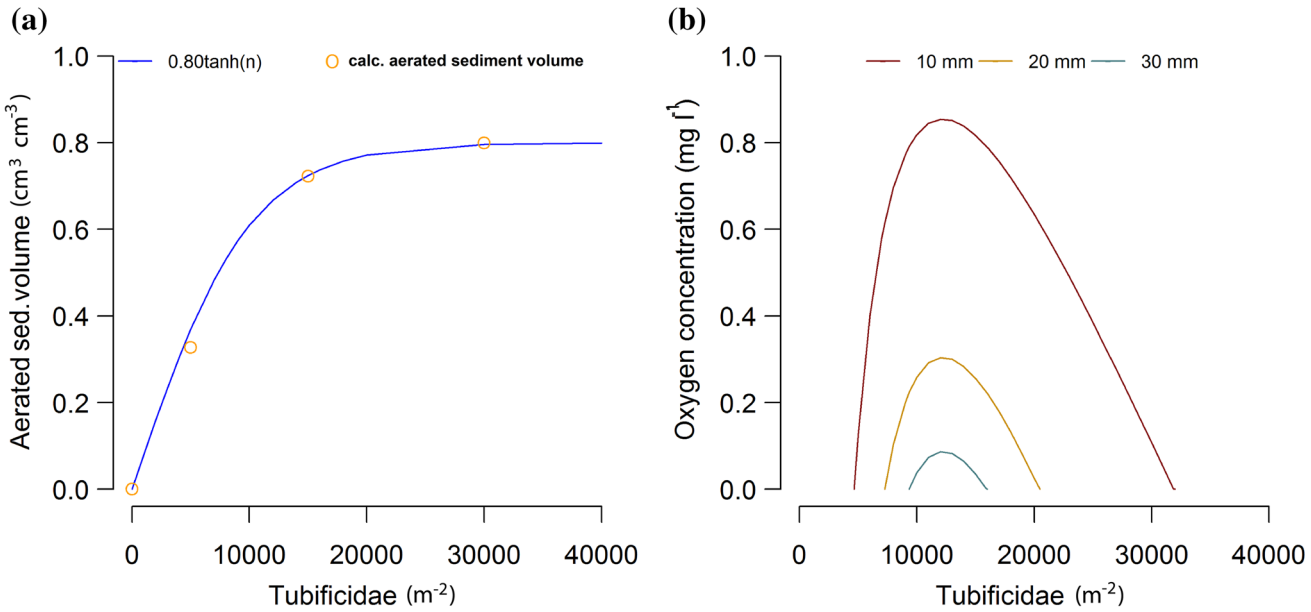

Fig. 4 **a** Calculated average aerated sediment volume (cm^3) for T_{5k}, T_{15k}, and T_{30k} (orange circles) and modeled aerated sediment volume (cm^3) per number of Tubificidae (m^{-2}) (dark blue) (**a**). **b** The modeled burrow function corresponds to a tangent-hyperbolic function (0.80 tan h(n)) and was used to model oxygen concentration in the sediment (mg l^{-1}) per number of Tubificidae (m^{-2}) for three different depths: 10 mm (red), 20 mm (yellow) and 30 mm (blue)

factor analysis (Table 2). Tubificidae at a density of 30,000 worms m^{-2} required more oxygen than was made available by aeration. Note that although this density is apparently not suitable for optimizing oxidation in Markermeer sediments, these high densities do occur in reality, especially in organically enriched environments and waste water (e.g. Nogaro et al. 2009).

The aeration effect of bioturbating Tubificidae effectively altered biogeochemical processes in the upper layer of the sediment, thereby influencing nutrient availability. Both NH_4 and NO_x concentrations increased in all treatments (Fig. 2c, d). The accumulation of nitrate in the upper layer of the sediment is most likely a result of aerobic oxidation of an upward flux of NH_4 (Anschutz et al. 2012), i.e., the supply of oxygen into the sediment was large enough to promote nitrification. The difference in average NH_4 concentrations between T_{15k} (0.70 mg l^{-1}) and T_{30k} (1.77 mg l^{-1}) is remarkable and suggests enhanced ammonification in T_{30k}. Since organic matter content in these sediments is low (Saaltink et al. 2018), ammonification suggests that the Tubificidae at a density of 30,000 worms m^{-2} required more oxygen than was made available by aeration. Moreover, decomposition of

dead Tubificidae may occur at a fast rate in bioturbated sediments, as bioturbation enhances microbial activity (Hansen and Kristensen 1997), further explaining the increased NH_4 concentrations in the upper 50 mm of the sediment in T_{30k}. Hence, treatments containing 5000 and 15,000 worms m^{-2} effectively increased N availability in the sediment and in the water column. At a density of 30,000 worms m^{-2}, however, the increased N concentrations are likely caused by decomposition of the introduced Tubificidae themselves. Therefore, the largest effect of bioturbation on the N concentrations in the sediment and the water column of lake Markermeer was found for a Tubificidae density at 15,000 worms m^{-2}.

In contrast to N, a negative effect was found for P; bioturbation decreased P concentrations in the sediment (Fig. 2b). Furthermore, no exchange of P with the water column was identified. This immobilization effect was mainly visible in the upper 16 mm of the sediment and is also explained by enhanced oxidation. The effect of P immobilization strongly depends on the geochemical composition of the sediment. For example, a positive upward flux of P to the water column was reported by Scicluna et al. (2015) and Zhu et al. (2016), especially after periods of hypoxia. Such P retention and release effects become especially important when significant amounts of iron-bound phosphorus are present in the sediment. As the sediment used in this experiment is rich in iron-bound phosphorus and pyrite (40 mg kg^{-1} for iron bound phosphorus and 10,000 mg kg^{-1} for pyrite; Table 1), it is not surprising, therefore, that the P concentration in the sediment decreased when oxygen concentrations increased. This is in concordance with the geochemical model simulations presented in this study (Table 3). Pyrite oxidation with associated calcite dissolution were identified as dominant geochemical processes induced by bioturbating Tubificidae. Oxidation of pyrite (FeS_2) is directly coupled to immobilization of P via precipitation of iron hydroxy phosphates (Table 3), which can occur upon aeration of pH-neutral and PO_4 rich groundwater (Griffioen 2006; Van der Grift et al. 2016). Van de Velde and Meysman (2016) showed that bioturbation indeed improves the recycling of Fe and S between their reduced and oxidized states. From a sediment depth of 21 mm onwards, no clear effect on the P concentration was found between the treated and the control samples, with P concentrations at 51 mm ranging from 4 mg l^{-1} in T_{15k} to 9 mg l^{-1} in T_{5k}. This indicates that the oxidation effect of bioturbation below 21 mm did not have a distinct impact on geochemical processes associated with P availability.

Since the macrofauna density in lake Markermeer currently amounts to about 12,800 individuals m^{-2} (of which about 5500 m^{-2} are Annelida), colonizing the sediment in the littoral zone of the created wetlands with about 7000 Tubificidae m^{-2} might enhance initial ecosystem development due to improved availability of N. However, when macroinvertebrates other than Annelida partly aerate the sediment, colonizing the sediment at a lower density is preferred. Fast initial ecosystem development is crucial when wetlands are constructed with soft mud as aboveground plant biomass dampens erosive stresses on the substrate by attenuating waves (Nepf 2012). Although the outcome of this experiment provides valuable information for developing ecological engineering practices, a direct translation into practical measures to be implemented is difficult due to several limitations related to the set-up of the experiment. First, it must be noted that the precise effect of colonization by Tubificidae into the littoral zone is hard to predict, as in reality, hydrodynamic factors also determine sediment oxidation, such as wave action with associated resuspension and settling. However, Volkenborn et al. (2007) showed that the effect of bioturbation on geochemical processes in aquatic systems is even visible in physically dominated systems, such as the Wadden Sea. Second, the experimental sediment only contained Tubificidae, whereas in reality interactions with other macro invertebrates exist. How such interactions in sediment from lake Markermeer might influence nutrient availability remains unknown. Last, the oxidation effect of bioturbation partly depends on the oxygen concentration in the lake. These concentrations show seasonal variation from 8 mg l^{-1} in summer to 14 mg l^{-1} during winter (Ministry of Infrastructure and the Environment 2017). Thus, the oxidation effect of bioturbation is larger in winter and spring than in summer and autumn (Supplementary Fig. 2). The aforementioned factors might explain the current density of Tubificidae present in lake Markermeer sediments (3900 Tubificidae m^{-2}). Despite these limitations, this study clearly showed significant effects of bioturbation by Tubificidae on sediment aeration and associated nutrient availability in the porewater and water column.

Acknowledgements This study was supported with funding from Netherlands Organization for Scientific Research (NWO), Stichting voor de Technische Wetenschappen (project no. 850.13.032) and the companies Deltares, Boskalis and Van Oord. This manuscript was produced with unrestricted freedom to report all results. We would also like to express our thanks to Thom Claessen and John Visser for their help, support and advice during the experiment.

References

Anschutz P, Ciutat A, Lecroart P, Gérino M, Boudou A (2012) Effects of Tubificid worm bioturbation on freshwater sediment biogeochemistry. Aquat Geochem 18:475–497

Callender E, Hammond DE (1982) Nutrient exchange across the sediment–water interface in the Potomac River estuary. Estuar Coast Shelf Sci 15:395–413

De Lucas Pardo MA (2014) Effect of biota on fine sediment transport processes. A study of lake Markermeer. Ph.D. dissertation, Delft University

De Lucas Pardo MA, Bakker M, Van Kessel T, Cozzoli F, Winterwerp JC (2013) Erodibility of soft freshwater sediments in Markermeer:

the role of bioturbation by meiobenthic fauna. Ocean Dyn 63:1137–1150
Egozcue JJ, Pawlowsky GV, Mateu Figueras F, Barceló Vidal C (2003) Isometric logratio transformations for compositional data analysis. Math Geol 35:279–300
Fillos J, Swanson WR (1975) The release rate of nutrients from river and lake sediments. Water Pollut Control Fed J 47:1032–1042
Filzmoser P, Hron K, Reimann C, Garret RG (2009) Robust factor analysis for compositional data. Comput Geosci 35:1854–1861
Fisher B, Lick WJ, McCall PL, Robbins JA (1980) Vertical mixing of lake sediments by tubificid oligochaetes. J Geophys Res 85:3997–4006
Fowler DJ, Goodnight CJ (1965) The effect of environmental factors on the respiration of *Tubifex*. Am Midl Nat 74:418–428
Griffioen J (2006) Extent of immobilization of phosphate during aeration of nutrient-rich, anoxic groundwater. J Hydrol 320:359–369
Han P, Bartels DM (1996) Temperature dependence of oxygen diffusion in H_2O and D_2O. J Phys Chem 100:5597–5602
Hansen K, Kristensen E (1997) Impact of macrofaunal recolonization on benthic metabolism and nutrient fluxes in a shallow marine sediment previously overgrown with macroalgal mats. Estuar Coast Shelf Sci 45:613–628
Helder W, De Vries RTP (1979) An automatic phenol-hypochlorite method for the determination of ammonia in sea- and brackish waters. Neth J Sea Res 13:154–160
Iversen N, Jørgensen BB (1993) Diffusion coefficients of sulfate and methane in marine sediments: influence of porosity. Geochim Cosmochim Acta 57:571–578
Kitson RE, Mellon MG (1944) Colorimetric determination of phosphorus as molybdivanadophosphoric acid. Ind Eng Chem Anal Ed 16:379–383
Krantzberg G (1985) The influence of bioturbation on physical, chemical and biological parameters in aquatic environments: a review. Environ Pollut 39:99–122
Kristensen E (2000) Organic matter diagenesis at the oxic/anoxic interface in coastal marine sediments, with emphasis on the role of burrowing animals. Hydrobiologia 426:1–24
Kristensen E, Penha-Lopes G, Delefosse M, Valdemarsen T, Quintana CO, Banta GT (2012) What is bioturbation? The need for a precise definition for fauna in aquatic sciences. Mar Ecol Prog Ser 446:285–302
Lagauzère S, Moreira S, Koschorreck M (2011) Influence of bioturbation on the biogeochemistry of littoral sediments of an acidic post-mining pit lake. Biogeosciences 8:339–352
Lobet G, Pagès L, Draye X (2011) A novel image analysis toolbox enabling quantitative analysis of root system architecture. Plant Physiol 157:29–39
Lou J, Cao Y, Sun P, Zeng P (2013) The effects of operational conditions on the respiration rate of Tubificidae. PLoS One 8:1–9
Luedecke C, Hermanewicz SW, Jenkins D (1989) Precipitation of ferric phosphate in activated sludge: a chemical model and its verification. Water Sci Technol 21:325–337
Martin P, Boes X, Goddeeris B, Fagel N (2005) A qualitative assessment of the influence of bioturbation in Lake Baikal sediments. Glob Planet Change 46:87–99
Mermillod-Blondin F, Rosenberg R (2006) Ecosystem engineering: the impact of bioturbation on biogeochemical processes in marine and freshwater benthic habitats. Aquat Sci 68:434–442
Ministry of Infrastructure and the Environment (2017) Watergegevens Rijkswaterstaat. http://watergegevens.rws.nl/. Accessed 11 Oct 2017
Mitsch WJ (1998) Ecological engineering—the 7-year itch. Ecol Eng 10:119–130
Nepf HM (2012) Flow and transport in regions with aquatic vegetation. Annu Rev Fluid Mech 44:123–142
Nogaro G, Mermillod-Blondin F, Valett MH, François-Carcaillet F, Gaudet JP, Lafont M, Gibert J (2009) Ecosystem engineering at the sediment–water interface: bioturbation and consumer–substrate interaction. Oecologia 161:125–138
Noordhuis R, Groot S, Dionisio Pires M, Maarse M (2014) Wetenschappelijk eindadvies ANT-IJsselmeergebied. Vijf jaar studie naar kansen voor het ecosysteem van het IJsselmeer, Markermeer en IJmeer met het oog op de Natura-2000 doelen. Deltares report 1207767-000
Oates BR (1985) Photosynthesis and amelioration of desiccation in the intertidal saccate alga *Colpomenia peregrina*. Mar Biol 89:109–119
Odum HT, Odum B (2003) Concepts and methods of ecological engineering. Ecol Eng 20:339–361
Parkhurst DL, Appelo CAJ (2013) Description of input and examples for PHREEQC version 3-A computer program for speciation, batch-reaction, one-dimensional transport, and inverse geochemical calculations. U.S. Geological Survey, Denver
Pelegri SP, Blackburn TH (1995) Effects of *Tubifex tubifex* (Oligochaeta: Tubificidae) on N-mineralization in freshwater sediments, measured with 15N isotopes. Aquat Microbiol Ecol 9:289–294
Rogaar H (1980) The morphology of burrow structures made by Tubificids. Hydrobiologia 71:107–124
Ruginis T, Bartoli M, Petkuviene J, Zilius M, Lubiene I, Laini A, Rainkovas-Baziukas A (2014) Benthic respiration and stoichiometry of regenerated nutrients in lake sediments with *Dreissena polymorpha*. Aquat Sci 76:405–417
Saaltink RM, Dekker SC, Griffioen J, Wassen MJ (2016) Wetland eco-engineering: measuring and modeling feedbacks of oxidation processes between plants and clay-rich material. Biogeosciences 13:4945–4957
Saaltink RM, Dekker SC, Eppinga MB, Griffioen J, Wassen MJ (2017) Plant-specific effects of iron toxicity in wetlands. Plant Soil 416:83–96
Saaltink RM, Dekker SC, Griffioen J, Wassen MJ (2018) Vegetation growth and sediment dynamics in a created freshwater wetland. Ecol Eng 111:11–21
Sanford LP (2008) Modeling a dynamically varying mixed sediment bed with erosion, deposition, bioturbation, consolidation, and armoring. Comput Geosci 34:1263–1283
Schaller J (2014) Bioturbation/bioirrigation by *Chironomus plumosus* as main factor controlling elemental remobilization from aquatic sediments? Chemosphere 107:336–343
Scicluna TR, Woodland RJ, Zhu Y, Grace MR, Cook PLM (2015) Deep dynamic pools of phosphorus in the sediment of a temperate lagoon with recurring blooms of diazotrophic cyanobacteria. Limnol Oceanogr 60:2185–2196
Svensson JM, Leonardsson L (1996) Effects of bioturbation by tube-dwelling chironomid larvae on oxygen uptake and denitrification in eutrophic lake sediments. Freshw Biol 35:289–300
Svensson JM, Enrich-Prast A, Leonardson L (2001) Nitrification and denitrification in a Eutrophic Lake sediment bioturbated by oligochaetes. Aquat Microb Ecol 23:177–186
Temmerman S, Meire P, Bouma TJ, Herman PMJ, Ysebaert T, de Vriend HJ (2013) Ecosystem-based coastal defence in the face of global change. Nature 504:79–83
Turner CB (2010) Influence of zebra (*Dreissena polymorpha*) and quagga (*Dreissena rostriformis*) mussel invasions on benthic nutrient and oxygen dynamics. Can J Fish Aquat Sci 67:1899–1908
Ullman WJ, RC Aller (1981) Diffusion coefficients in nearshore marine sediments. Limnol Oceanogr 27:552–556
Van Kessel T, De Boer G, Boderie P (2008) Calibration suspended sediment model Markermeer. Open File Rep 4612:107 pp

Van Riel MC, Verdonschot PFM, Dekkers DD (2018) De bodemfauna van het Markermeer. Markermeer bodemfaunakartering 2016 en MWTL-analyse. https://doi.org/10.18174/442521

Van de Velde S, Meysman FJR (2016) The influence of bioturbation on iron and sulphur cycling in marine sediments: a model analysis. Aquat Geochem 22:469–504

Van der Grift B, Behrends T, Osté LA, Schot PP, Wassen MJ, Griffioen J (2016) Fe hydroxyphosphate precipitation and Fe(II) oxidation kinetics upon aeration of Fe(II) and phosphate-containing synthetic and natural solutions. Geochim Cosmochim Acta 186:71–90

Vepraskas MJ, Polizzotto M, Faulkner SP (2001) Redox chemistry of hydric soils in wetland soils: genesis, hydrology, landscapes, and classification. CRC Press, Boca Raton

Vijverberg T, Winterwerp JC, Aarninkhof SGJ, Drost H (2011) Fine sediment dynamics in a shallow lake and implication for design of hydraulic works. Ocean Dyn 61:187–202

Vink JPM (2002) Measurement of heavy metal speciation over redox gradients in natural water–sediment interfaces and implications for uptake by benthic organisms. Environ Sci Technol 36:5130–5138

Vink JPM (2009) The origin of speciation: trace metal kinetics and bioaccumulation by oligochaetes and chironomids in undisturbed water–sediment interfaces. Environ Pollut 157:519–527

Volkenborn N, Polerecky L, Hedtkamp SIC, van Beusekom JEE, de Beer D (2007) Bioturbation and bioirrigation extend the open exchange regions in permeable sediments. Limnol Oceanogr 52:1898–1909

Walker RA, Hallock P, Torres JJ, Vargo GA (2011) Photosynthesis and respiration in five species of benthic Foraminifera that host algal endosymbionts. J Foramin Res 41:314–325

Zhu Y, Hipsey MR, McCowan A, Beardall J, Cook PLM (2016) The role of bioirrigation in sediment phosphorus dynamics and blooms of toxic cyanobacteria in a temperate lagoon. Environ Model Softw 86:277–304